Separation and Purification Technology 401 (2026) 138507

Contents lists available at ScienceDirect

Separation and Purification Technology

journal homepage: www.elsevier.com/locate/seppur

Hexavalent chromium (Cr(VI)) removal by reduction-coagulation-filtration (RCF) combined with deacidification in drinking water treatment: A pilot study

Oliver Dördelmann [a], Stefan Hahn [a], Mohammad Al-Ameer Abadi [b], Stefan Panglisch [b,c], Daniel Mahringer [d,*]

[a] IWW Analytik und Service GmbH, Moritzstr. 26, 45476 Mülheim an der Ruhr, Germany
[b] University of Duisburg-Essen (UDE), Faculty Engineering Sciences, Mechanical Process Engineering/Water Technology, Lotharstr. 1, MF 164, 47057 Duisburg, Germany
[c] IWW Institut für Wasserforschung gemeinnützige GmbH, Moritzstr. 26, 45476 Mülheim an der Ruhr, Germany
[d] German Environment Agency, Section II 3.3 Water Treatment, Schichauweg 58, 12307 Berlin, Germany

ARTICLE INFO

Editor name: V Tarabara.

Keywords:
Hybrid process
Semi-technical experiment
limestone filtration
Fe(II) dosage
Cr(III) precipitation
Kinetics

ABSTRACT

Excess dissolved carbon dioxide (CO_2) is frequently encountered in natural groundwaters, originating from both geochemical and biological processes. In the investigated case, contamination of groundwater with toxic hexavalent chromium (Cr(VI)) occurred due to anthropogenic activities. The co-occurrence of CO_2 and Cr(VI) posed a distinct challenge for water treatment, as multiple process steps need to be tailored to remove both substances at the same time. This study investigates an integrated treatment approach specifically developed for groundwater containing elevated levels of both Cr(VI) and CO_2. The process combines reduction coagulation filtration (RCF) with ferrous iron (Fe(II)) dosage with limestone filtration for concurrent Cr(VI) removal and water deacidification. A pilot plant with two parallel filters—one filled with dense limestone and the other with porous limestone—was operated under varying Fe(II) dosages (Fe(II), 0.3–1.0 mg/L) and filtration velocities (4.4–15.5 m/h). Results demonstrate that the RCF process achieved efficient Cr(VI) removal at moderate Fe(II) concentrations (<1.0 mg/L), with no breakthrough or reoxidation observed. Limestone filtration efficiently increased pH, calcium concentration, and buffer capacity, thereby decarbonating the water. Porous limestone showed higher reactivity than the dense limestone commonly used. Analysis of backwash sludge confirmed stable chromium retention and low residual metal concentrations in the supernatant. These findings confirm that the integrated RCF–limestone process provides an effective and cost-efficient solution for treating groundwater impacted by anthropogenic Cr(VI) and naturally elevated CO_2 concentration.

1. Introduction

Hexavalent chromium (Cr(VI)) is a toxic contaminant occasionally detected in drinking water sources worldwide, originating mostly from natural geogenic processes or potentially from anthropogenic activities [1,2]. The World Health Organization (WHO) declared a provisional guideline value for total chromium in drinking water of 50 µg/L [3] and the European Drinking Water Directive will implement a limitation value of 25 µg/L from 2036 onwards [4]. The German Drinking Water Ordinance will lower the current limitation value of 25 µg/L further down to 5 µg/L from 2030 onwards [5]. California introduced a limitation value of 10 µg/L for Cr(VI) in 2024 [6].

Over the entire pH range Cr(VI) occurs as dominant oxidation species for high oxidation reduction potentials (ORP) while Cr(III) occurs at low ORP (Fig. S1). Due to its high mobility in aquatic systems and severe health implications effective Cr(VI) removal from drinking water is imperative [7,8]. Conventional treatment methods for Cr(VI) removal include adsorption, ion exchange, and membrane filtration, but these techniques often face limitations such as high operational costs, secondary waste generation, or inefficiency at low concentrations [9]. The treatment combination reduction, coagulation and filtration (RCF) is a promising alternative, where Cr(VI) is first reduced by addition of Fe(II) to the less toxic and less soluble trivalent form (Cr(III)), followed by coagulation and filtration [10–12].

* Corresponding author.
E-mail address: daniel.mahringer@uba.de (D. Mahringer).

https://doi.org/10.1016/j.seppur.2026.138507
Received 2 March 2026; Received in revised form 24 April 2026; Accepted 14 May 2026
Available online 17 May 2026

Many natural groundwater sources have pH values below the target required by national drinking water regulations. Acid-forming processes—such as the oxidation of iron and manganese, hydrogen sulfide, and ammonium—make groundwater treatment necessary to raise the pH. In Germany, drinking water must have a pH between 6.5 and 9.5, and the calcite dissolution capacity must not exceed 5 mg/L $CaCO_3$. If the pH is above 7.7, this requirement is automatically fulfilled; for pH values below 7.7, it must be demonstrated by calculation that the calcite dissolution capacity remains below 5 mg/L $CaCO_3$ [5].

1.1. Deacidification processes

Deacidification processes are used to adjust the desired CO_2 concentration or a specific pH value in water. Depending on the water quality and the deacidification objective, a distinction is made between physical processes, such as filtration using alkaline filter materials and the dosing of chemicals. In the case of very soft water, hardening can be advantageous. To achieve this, in some cases it can be useful to first add carbon dioxide to the water. Filtration using alkaline filter materials or the dosing of calcium hydroxide increases the water's content of alkaline earth and hydrogen carbonate ions. The preferred deacidification methods primarily depend on the raw water quality (CO_2-acidity and total alkalinity) and the desired drinking water quality (e.g. total alkalinity and hardness) [13].

Water with a total alkalinity above 1.5 mmol/L can typically be deacidified by mechanical methods alone, which involve stripping of dissolved CO_2 by aeration. For waters with total alkalinity between 1.0 and 2.0 mmol/L, mechanical deacidification can raise pH to 7.7 or above. However, in waters with total alkalinity greater than 2.0 mmol/L, calcium carbonate precipitation may occur due to undershooting the CO_2 equilibrium. Waters with total alkalinity below 1.0 mmol/L generally require chemical deacidification—such as limestone filtration—to reach the target pH. High CO_2-acidity may require an initial mechanical partial deacidification step, sometimes combined with hardening (increasing calcium and alkalinity) prior to mechanical treatment. The process design must consider these factors carefully to ensure regulatory compliance and optimal water quality [13–15].

1.2. Background of the pilot plant investigations

The pilot plant investigations were conducted for a German water utility that uses groundwater from various wells for drinking water supply. The raw water is soft and has a low pH value of 6.0–6.2. Until now, deacidification has been the only treatment goal. The existing waterworks uses milk of lime (a suspension of calcium hydroxide) for deacidification, followed by sand filtration. In recent years, however, there have been several operational problems in the treatment plant, mainly caused by lime precipitation in pipes and valves. Moreover, Cr (VI) contamination has been detected in the catchment area. For these reasons, the respective water utility would like to build a new drinking water treatment plant that also includes an option for Cr(VI) removal. A particular challenge is the limited space available at the waterworks site. Therefore, a compact treatment process with a small footprint had to be developed.

In these investigations, the total alkalinity of the raw water was below 1.0 mmol/L and the CO_2-acidity was comparatively high. Therefore, a combination of a) limestone filtration for CO_2 consumption, HCO_3^- development, pH increase and hardening followed by b) mechanical aeration for additional CO_2 stripping and fine adjustment of pH was chosen as the deacidification measures. This combination allows for a low residence time in the limestone filters, resulting in compact filters. An insufficient pH increase in the limestone filters can be compensated for by subsequent mechanical deacidification. German technical guidelines recommend this process combination for the deacidification of very soft and acidic groundwater [15].

The increases of calcium and total alkalinity (mainly the concentration of HCO_3^-) and decrease of CO_2-acidity during limestone filtration can be described according to the following equation:

$$CO_2 + CaCO_3 + H_2O \leftrightarrow Ca^{2+} + 2\,HCO_3^- \quad (1)$$

As the equation shows an equilibrium, addition of CO_2 (on the left side) will push the equilibrium to the right side. Therefore, the pilot plant included an optional dosage of CO_2 as booster prior to limestone filtration for hardness and HCO_3^- adjustment. Increase of pH, e.g. by addition of a base, would push the equilibrium to the left side, whereas decrease of pH, e.g. by addition of an acid, would push the equilibrium to the right side.

1.3. Reduction kinetics of Cr(VI) with Fe(II) in a technical system for RCF

The reduction kinetics of Cr(VI) by Fe(II) in a drinking water treatment relevant pH range are strongly governed by pH, with rates increasing significantly from circumneutral to slightly alkaline conditions due to the progressive existence of hydrolyzed Fe(II) species, specifically $Fe(OH)^+$ and $Fe(OH)_2(aq)$ [16,17]. Elevated temperatures, within the typical range of groundwater sources, further accelerate the reaction rate through a thermodynamically driven shift in Fe(II) speciation favoring these same reactive hydrolyzed forms [17]. Dissolved oxygen is a competing oxidation agent for Fe(II) oxidation, however Cr (VI) is kinetically favored below a pH of 10 above which oxidation of Fe (II) is faster by dissolved oxygen than Cr(VI). [18]. Additionally, the observed pseudo-first-order dependence on Cr(VI) concentration confirms that the reaction rate is directly proportional to the initial Cr(VI) concentration and is substantially accelerated by the elevated Fe(II) excesses commonly applied in reductive filtration processes [19,20].

1.4. Objectives of the pilot plant investigations

Anthropogenic groundwater contamination with Cr(VI) is a widespread environmental problem. When Cr(VI) occurs in soft and acidic waters, several goals must be achieved in drinking water treatment: removal of Cr(VI), deacidification, decrease in calcite dissolution capacity, and increase in hardness and buffer capacity. Whether these goals can be effectively achieved in a single filtration step was identified as an open research question, which was addressed in this study. RCF treatment for Cr(VI) removal was combined with limestone filtration for deacidification. The aim of the deacidification unit was to neutralize the pH, increase the buffer capacity and reduce the calcite dissolution capacity without impairment of the Cr(VI) removal. The novelty of the study is the combination of Cr(VI) removal using the RCF process with deacidification using limestone filtration in a single filtration step. The validation of this treatment combination was performed by experiments at semi-technical scale to guarantee up-scalability into technical scale.

The objectives of this study were (1) to evaluate the effectiveness of simultaneous Cr(VI) removal and deacidification during limestone filtration combined with RCF, (2) to optimize the combined process in terms of Fe(II) dosage and filtration velocity, (3) to evaluate the remobilization potential of chromium from the backwash sludge, (4) to evaluate conductivity as a surrogate parameter for monitoring and controlling deacidification.

The results of these pilot plant investigations will now be incorporated into the planning process for the new waterworks. Although this combination of treatment goals (chromium removal and deacidification) is relatively rare, it may also be a treatment option for other water suppliers.

2. Materials and methods

2.1. Chemicals

Dense and porous limestones were used as filter materials (Table 1).

Table 1
Filter material characteristics.

Filter material	Product	Grain size in [mm]	Bulk density in [kg/m^3]	Producer
Dense limestone	Jura Perle	1.0–2.0	1400	Eduard Merkle GmbH (Hamburg, Germany)
Porous limestone	Akdolit hydro-Calcit C G	0.5–3.15	1300	Lhoist Germany Rheinkalk GmbH, (Wuelfrath, Germany)

Ferrous sulfate heptahydrate (Avantor, Radnor, United States of America) of quality level 1 (DIN 889:2023), Hypochloric acid (product suprapure) from Merck, Darmstadt, Germany, and carbon dioxide pressure gas from Carbo Kohlensäurewerke, Bad Hönningen, Germany were used.

2.2. Water quality parameters

The water used during this study was the original groundwater of a drinking treatment water plant in the Rhineland (Germany). As the water works uses different wells, the raw water quality varies to some degree. The raw water concentrations are given in Table 2.

Cr(VI) and Cr_{total} concentrations in raw water were nearly identical throughout all experimental phases. This indicates that total chromium consisted almost exclusively of Cr(VI) in the samples, with only negligible differences observed between the two measurements. Minor discrepancies – e.g. 5.6 µg/L for Cr(VI) vs. 5.0 µg/L for chromium total - can be attributed to variations in analytical methods and measurement uncertainties. As the chromium concentrations sometimes are in the range of the future German limit value (5.0 µg/L), the water utility is aiming to remove chromium.

Given its low conductivity and low cation and anion concentrations, the groundwater can be characterised as weakly mineralised water. Unusually for German groundwater, iron and manganese were not present in the raw water. The pH value of the raw water was approx. 6.0 and the calcite dissolution capacity was well above 5 mg/L. Deacidification was therefore necessary in order to comply with the German Drinking Water Ordinance.

2.3. Target values

With regard to the German Drinking Water Ordinance the water quality goals for the effluent of the pilot plant were defined as follows:

- $Chromium_{total} < 2.5$ µg/L
- pH ≥ 7.7

A target value for total alkalinity is not included in the German Drinking Water Ordinance. However, in view of corrosion incidents in the distribution network of the respective water utility, a target value of ≥2.0 mmol/L has been set for total alkalinity.

Table 2
Raw water quality ($n = 19$).

Raw water parameter	Unit	Min	Max
pH	–	5.9	6.2
Conductivity	µS/cm	245	266
CO_2-acidity	mmol/L	0.9	1.2
Total alkalinity	mmol/L	0.5	0.9
Chloride	mg/L	17	25
Nitrate	mg/L	11	14
Sulphate	mg/L	34	41
Calcium	mg/L	20	24
Magnesium	mg/L	5.5	6.4
Sodium	mg/L	13	16
Potassium	mg/L	1	2
Iron total	mg/L	<0.010	<0.010
Manganese	mg/L	<0.010	<0.010
Total organic carbon (TOC)	mg/L	0.4	0.6
UV absorbance at 254 nm (SAC254)	1/m	0.2	0.7
Chromium total	mg/L	<0.5	5.0
Cr(VI)	mg/L	<0.02	5.6
Water hardness	mmol/L	0.73	0.88
Calcite dissolution capacity	mg/L $CaCO_3$	78	104

2.4. Pilot plant setup

The pilot plant was equipped with two parallel filters, each featuring a filter vessel diameter of 0.24 m, a vessel height of 3.0 m, a filter area of 0.045 m^2, a filter bed height of 2.3 m, and a bed volume of 0.104 m^3. The process flow diagram (Fig. 1) depicts a storage tank for the mixed raw water, followed by the designated Fe(II) dosing point for Cr(VI) removal. Raw water was blended from five groundwater wells differing in Cr(VI) concentration. Over time, changes in well configuration led to corresponding variations in Cr(VI) concentration in the blended influent. To suppress Fe(II) oxidation in the dosing tank, the pH of the Fe(II) stock solution was adjusted to 2.8 [21]. After pressurization by a pump (operating at 1–2 bar and a flow of 200–700 L/h per filter), the water was split between two parallel filter lines. Optionally, CO_2 (0.5–1.0 mmol/L) could be added upstream of the filters, as indicated in the process diagram for improved limestone dissolution. Filtration performance was monitored online based on differential pressure, turbidity, conductivity and pH value.

Filter 1 was filled with dense limestone (Jura Perle), filter 2 with porous limestone (Hydro-Calcit). Empty bed contact times (EBCT) based on filtration velocity are provided in Table S1. Sampling points were installed after the raw water storage tank (prior to Fe(II) dosing), immediately before the filter inlets, and after filtration. The effluent from each filter was collected separately and subjected to analysis. Filter backwashing was performed sequentially after 1–2 weeks of operation, starting with compressed air, followed by a combination of compressed air and filtrate and finally filtrate alone. Backwash water was collected, allowed to settle, and the supernatant sampled after 2 and 24 h of sedimentation.

Due to the short contact times in the limestone filters, the pH of the filter effluents frequently remained below 7.7, and the calcite dissolution capacity of the water exceeded the maximum allowable value prescribed by the German Drinking Water Ordinance (5 mg/L $CaCO_3$). Therefore, the effluents from both filters were combined and subjected to further treatment by mechanical deacidification. This process involved aerating the mixed water with a fan to strip excess CO_2. The fan speed could be adjusted to control the extent of CO_2 removal and, consequently, the effluent pH. After mechanical deacidification, samples were taken to determine pH, conductivity, and residual CO_2-acidity of the treated water.

2.5. Experimental procedure

During some phases of the pilot plant experiments Fe(II) was dosed into the mixed raw water at different concentrations (0.3 mg/L – 0.9 mg/L). The contact times between Fe(II)-dosage and filter bed entry are given in Table S2. For improved deacidification CO_2 dosing prior to the filters was possible. Different filtration velocities were tested (4.4 m/h – 15.5 m/h). The experiments were executed in five phases for 18 weeks in total (Table 3). The parameters Cr(VI), Cr_{total}, Fe(II), Fe_{total}, calcium and magnesium concentrations, conductivity, pH, turbidity, total alkalinity and CO_2-acidity were measured at the different sampling points (Fig. 1).

The spent filter backwash water was collected and allowed to settle without the addition of flocculants or flocculation aids. After 24 h of sedimentation, samples of both the supernatant and the settled sludge

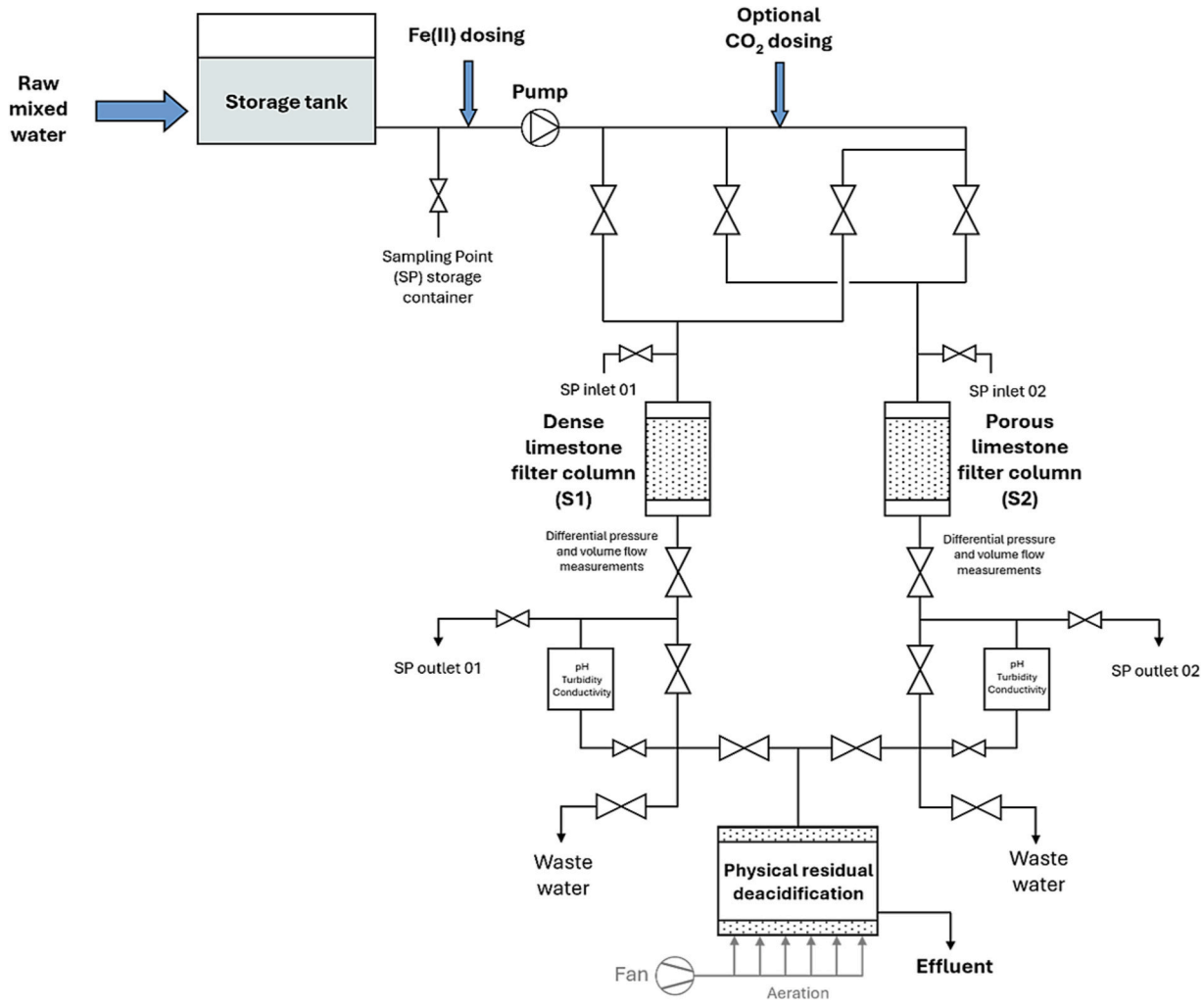

Fig. 1. Process flow diagram of the pilot plant

Table 3
Experimental phases.

Phase	Duration in weeks	CO_2 dosing concentration in mmol/L	Fe(II) dosage in mg/L iron	Filtration velocity in m/h	EBCT in min
Phase 1	6	–	–	8.8 successive decrease to 4.4	16 successive increase to 28
Phase 2	5	0.5–1.0	–	11.1 successive increase to 15.5	12 successive decrease to 9
Phase 3	4	–	0.4–0.9[a]	8.8 successive increase to 13.3	16 successive decrease to 10
Phase 4	2	0.5	0.3–0.4[a]	13.3 successive increase to 15.5	10 successive decrease to 9
Phase 5	1	–	–	10.4	10

[a] Dosage concentrations with respect to the experimental week during this phase are given in Table S2.

were collected to determine heavy metal concentrations and contents, respectively. The sedimented sludge was dried at 105 °C, homogenized, and a representative fraction was weighed and subjected to aqua regia digestion. The resulting solution was then analyzed for heavy metal content.

2.6. Analytics

Conductivity and pH were measured on-site using Multi 3630 IDS electrodes (Xylem Analytics, Weilheim, Germany). Alkalinity and acidity were determined via titration with a Robotic Titrosampler (Metrohm, Filderstadt, Germany). Turbidity was assessed on-site with a Lovibond TB 250 nephelometric meter (Tintometer, Dortmund, Germany) and monitored online after each filtration with Ultraturb devices (Hach Lange, Düsseldorf, Germany). Concentrations of calcium, magnesium, sodium, potassium, total chromium, manganese and iron were analyzed by inductively coupled plasma optical emission spectroscopy (ICP-OES; Optima 8000, Perkin Elmer, USA) with a quantification limit of 0.5 µg/L. Cr(VI) was quantified by liquid chromatography coupled with inductively coupled plasma mass spectrometry (LC-ICP-MS; Agilent 7900, Agilent, USA), with a quantification limit of 20 ng/L. Chloride, nitrate and sulphate were analyzed by ion chromatography (930 Compact IC Flex, Metrohm, Switzerland) with a quantification limit of 1.0 mg/L. TOC was measured with a NDIR-detector (TOC-L-series instrument, Shimadzu, Japan) with a quantification limit of 0.1 mg/L.

The calcite dissolution capacity was calculated according to the method described by Johannsen [22].

3. Results and discussion

3.1. Cr(VI) removal

Fig. 2 shows the Cr(VI) and total chromium concentrations in the inflow and outflow of filters 1 and 2 in the five different test phases. Depending on the configuration of the five groundwater wells, which had different chromium concentrations, the resulting concentration in the mixed raw water changed accordingly. During experimental phases 1 and 2, Fe(II) was not dosed, resulting in no chromium removal and, consequently, identical chromium concentrations in the influent and effluent.

In phase 3, the well configuration was adjusted to provide a high chromium influent concentration. During this phase, Fe(II) was dosed at 0.5 mg/L in the first week and dosage was increased to 1.0 mg/L during the following three weeks. In these phases Cr(VI) was reduced by Fe(II) to barely soluble Cr(III) in the supernatant of the filter where subsequently after reduction co-precipitates consisting of Fe(III)-Cr(III) hydroxide were formed [23]. These precipitates could be completely removed in the deep-bed limestone filters and hence the removals of Cr (VI) and Cr_{total} were identical. No breakthrough or reoxidation of Cr(III) was observed. Increasing the filtration velocity in phase 3 from 8.8 m/h to 13.3 m/h did not impair chromium removal efficiency, even as influent chromium concentrations rose from 2.4 µg/L to 4.6 µg/L due to changes in well configuration. A Fe(II) dose of 0.9 mg/L was sufficient to achieve complete chromium removal. The parameters Fe(II) concentration and pH value were described in literature as key driver for fast Cr (VI) reduction [19,20,22,23]. At higher pH hydrolyzed Fe(II) species improve reduction kinetics of Cr(VI). Even though pH of the influent was low (between 5.9 and 6.2) Cr(VI) reduction in the supernatant of the filters was sufficient. Fe(II) dosage of 0.9 mg/L compensated for the low kinetics of Cr(VI) reduction caused by the low pH value. Sampling along the filters was not possible, but it seems plausible that if Fe(II) entered the filter and pH increase caused by limestone dissolution occurred immediately after filter bed entry (as is expected), Cr(VI) reduction kinetics might have been positively influenced by the sudden pH increase, possible at the surface of the filter material where high pH increases are expected.

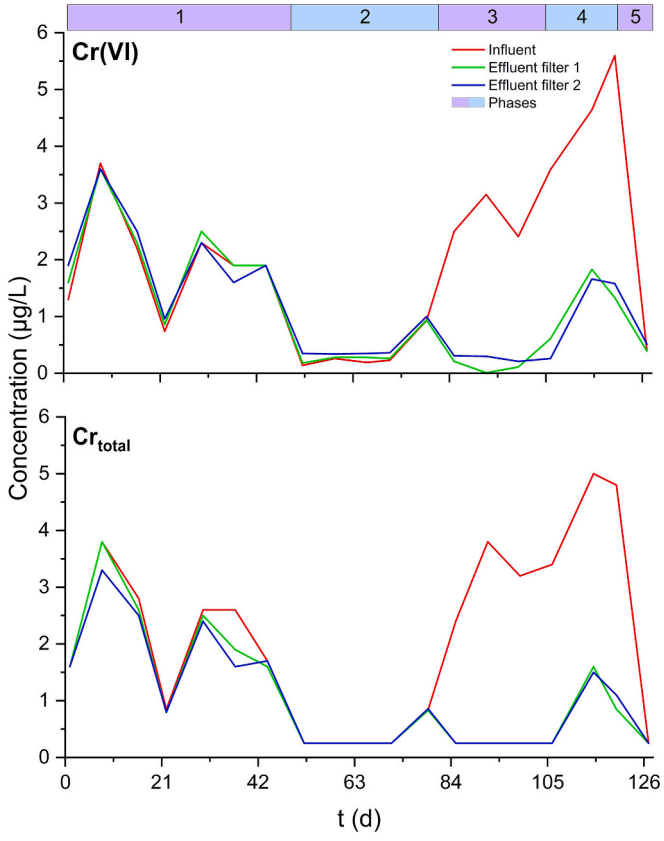

Fig. 2. Influent and effluent concentrations of Cr(VI) (top) and Cr_{total} (bottom).

Phase 4 was designed to represent worst-case conditions, featuring high filtration velocities (13.3–15.5 m/h), low Fe(II) dosages (0.3–0.4 mg/L), and elevated chromium influent concentrations (4.8–5.0 µg/L). This resulted in contact times in the filter supernatant of 3.1–3.6 min (Table S2). Under these circumstances, effluent concentrations of Cr(VI) and total chromium were detectable (Fig. 2 and Fig. S2), ranging from 1.0 to 1.5 µg/L, with total chromium comprised solely of Cr(VI) due to limited Cr(VI) reduction kinetics in the supernatant of the filter caused by low pH and low Fe(II) concentrations. In contrast, iron concentrations in the effluent were consistently below the limit of quantification, with the exception of a single measurement (23 µg/L), which remained well below the drinking water standard of 50 µg/L [24]. No iron breakthrough was expected because the increase of the pH during limestone filtration causes a speciation shift from unhydrolyzed to hydrolyzed Fe(II) species which are oxidised by dissolved oxygen very quickly to Fe(III) [25]. During all test phases, the turbidity of the filtrate was below 0.1 FNU. The absence of iron and turbidity breakthroughs at high filtration rates underlines the effectiveness of the biotic oxidation of Fe(II) to Fe(III) within the filters [26]. Although the molar excess of Fe (II) over Cr(VI) was approximately 100-fold, the Fe(II) dosage was apparently insufficient to completely reduce all Cr(VI) in the filter supernatant to Cr(III) within the short contact times, due to the low influent pH this finding was not surprising. The Fe(II) that was not oxidised in the supernatant but was quickly oxidised after entering the filter and then precipitated in the filter bed, due to the pH increase in the filter bed but also because of microbial catalysis within the deep-bed filter. After oxidation and precipitation iron was no longer available for further reactions with Cr(VI), resulting in a breakthrough of Cr(VI). However, the fraction of Cr(VI) that was reduced to Cr(III) in the supernatant was efficiently removed by the filter, despite the high filtration velocities, indicating high robustness of the deacidification filters towards turbidity breakthrough.

Since previous studies have demonstrated that a higher Fe(II) excess accelerates Cr(VI) reduction kinetics [16], increasing the Fe(II) dosage could have further reduced Cr(VI) concentrations in the filter supernatant, even within short contact times. Alternatively, extending the contact time in the supernatant at a constant Fe(II) dosage could enhance removal efficiency. This is generally achievable either by adding an additional contact tank or by reducing the filtration velocity. However, since filtration velocity did not negatively impact removal effectiveness (i.e., no Cr(III) breakthrough occurred), a higher Fe(II) dosage is advisable for improved Cr(VI) reduction, especially when installing an additional contact tank is not feasible or would be prohibitively expensive.

Chromium removal occurred immediately after the initiation of Fe (II) dosing in both filters and to an almost identical extent (Fig. 3). Cr(VI) was rapidly reduced to the sparingly soluble Cr(III) in the supernatant and co-precipitated with Fe(III) [23,27]. This finding indicates that the presence of Fe(II) in a sufficiently high excess over Cr(VI) is a crucial requirement for a successful RCF process. If present the chemical reduction of Cr(VI) occurs instantaneously.

3.2. Deacidification

Throughout all experimental phases, influent pH values varied slightly between 5.9 and 6.2, depending on well configurations (Table 2; Fig. 4, top). In phase 1, increasing the EBCT from 16 to 28 min in the filters resulted in higher effluent pH values for both filter 1 and filter 2. Conversely, in phase 3, successive reductions in EBCT led to decreasing effluent pH values. In phases 2 and 4, when CO_2 was dosed, effluent pH values were slightly lower compared to phases without CO_2 dosing; this

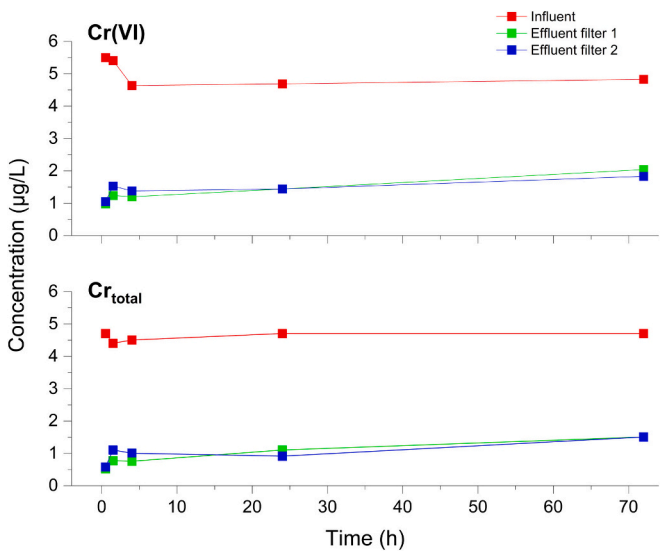

Fig. 3. Influent and effluent concentrations of Cr(VI) (top) and Cr_{tot} (bottom) after the start of Fe(II)-dosage.

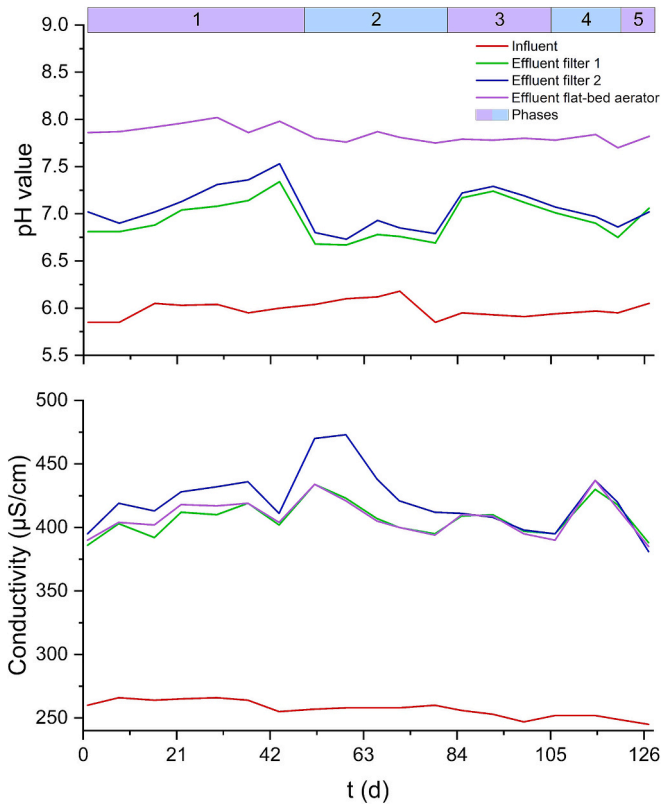

Fig. 4. Influent and effluent pH-values (top) and conductivity (bottom).

effect functioned as a "booster" for deacidification during filtration. As expected, further deacidification was achieved via post-filtration mechanical through stripping of excess CO_2 with air, yielding outlet pH values between 7.7 and 8.0.

The conductivity of the inflow remained virtually constant throughout the experiments ranging between 245 and 266 µS/cm (Table 2, Fig. 4, bottom). The highest conductivities of the effluent were observed during phases with CO_2-dosage before filtration in phases 2 and 4 due to increased dissolution of limestone. Conductivity increases were triggered by improved limestone dissolution and hence Ca^{2+} and HCO_3^- production during filtration as stated in eq. 1.

Influent calcium concentrations remained nearly constant between 20 and 24 mg/L, corresponding to water hardness values of 0.7 to 0.9 mmol/L (Table 2). Dissolution of the filter materials during limestone filtration increased both calcium concentration and water hardness in the effluents, resulting in calcium concentrations of 52–73 mg/L and water hardness values of 1.57–2.14 mmol/L (Fig. 5). Higher calcium concentrations and water hardness were observed in the effluent from filter 2, indicating greater reactivity of porous limestone compared to dense limestone. CO_2 dosing upstream of the filters (phases 2 and 4) led to enhanced dissolution of the filter materials (see eq. 1), and consequently increased Ca concentration, water hardness, and conductivity in the filter effluents (Fig. 4, bottom).

The influent alkalinity varied between 0.53 and 0.86 mmol/L (Table 2), which was considerably increased by limestone filtration (Fig. 6, top and middle). The alkalinity in the effluent of filter 2 (porous limestone) was slightly higher than that of filter 1 (dense limestone) throughout the experimental phases. Vice versa, the CO_2-acidity was decreased by the deacidification to a slightly higher amount for filter effluent 1. The CO_2-acidity after the mechanical deacidification was close to zero (compare Fig. 4, top with a pH close to 8.0). In phases 2 and 4 when CO_2 was dosed upstream of the filters, higher total alkalinity and CO_2-acidity were observed in the filter effluents.

The calcite dissolution capacity in the influent varied between 78 and 104 mg/L (Table 2), thus the raw water was highly limescale-dissolving. The limestone filters lowered the calcite dissolution capacity considerably with filter effluent 2 having been lowered further than filter effluent 1 (Fig. 6, bottom). The extent of reduction of the calcite dissolution capacities after filtration varied strongly between −2 and 60 mg/L. In the case of the slightly negative value the water was slightly limescale-separating. For almost all other cases the water needed further deacidification in order to comply with the requirements of the German Drinking Water Ordinance (5 mg/L $CaCO_3$) [24]. The additional treatment of mixed effluents with mechanical deacidification by aeration resulted in calcite dissolution capacities below 0 mg/L and hence limestone-separating. The dosage of CO_2 before the filters (phases 2 and 4) resulted in higher calcite dissolution capacities in the filter effluents than if no CO_2 was dosed, due to lower pH values though higher buffer capacity. By mechanical deacidification after limestone filtration almost calcite-depositing area was reached where the dissolved Ca^{2+} is precipitated to $CaCO_3$ because the of the exceedance of the solubility product of Ca^{2+} and CO_3^{2-}.

The deacidification reaction between CO_2 and limestone resulted in the creation of two mol bicarbonate (HCO_3^-) per created mol of Ca ion (compare eq. 1). Fig. 7 shows this relation if the molecular weight of Ca is considered. The figure also displays the slightly higher reactivity of Hydro-Calcit of filter two due to the higher slope of the fitted line.

The change in conductivity correlated with the change of Ca concentration (Fig. 8) and consequently the change in conductivity

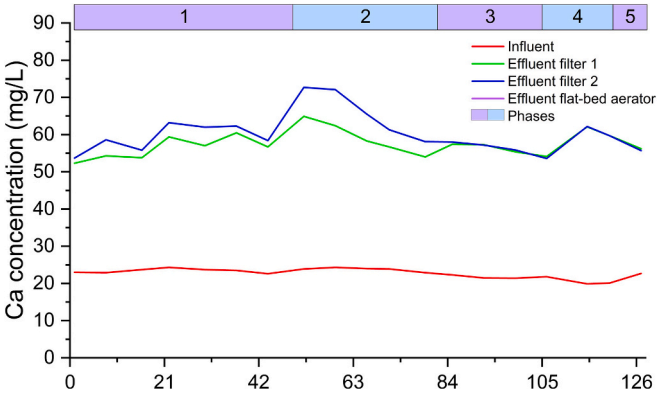

Fig. 5. Influent and effluent concentration of calcium.

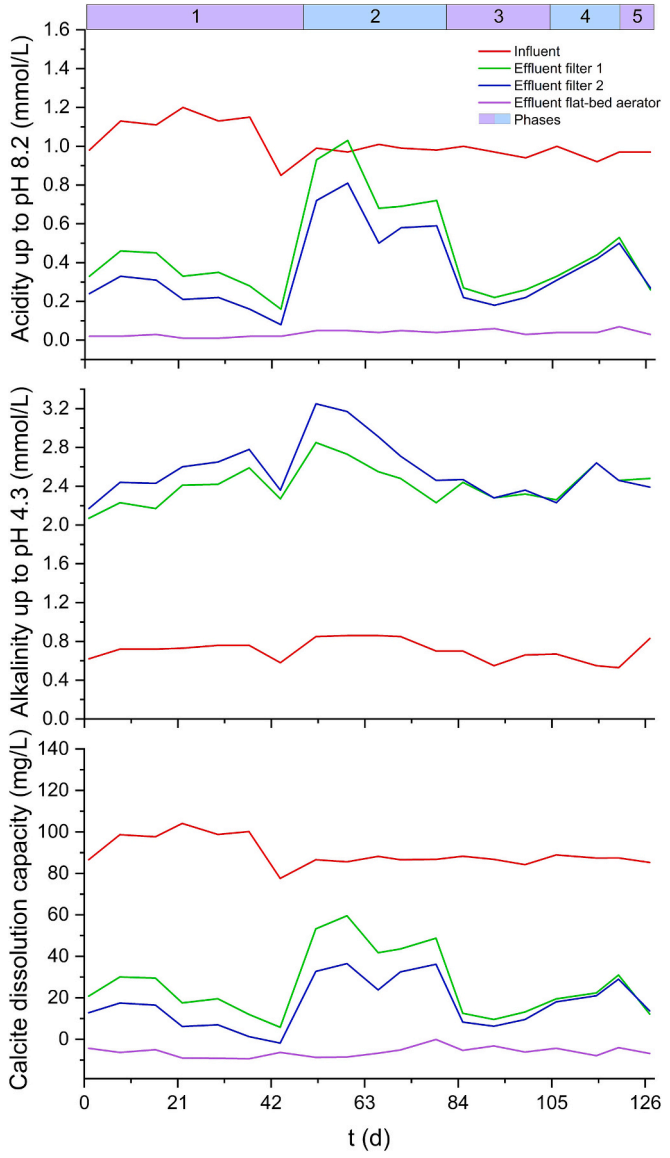

Fig. 6. CO_2-Acidity (top), total alkalinity (middle) and calcite dissolution capacity (bottom).

correlated with the change in alkalinity (Fig. 9). Due to the increase of the divalent Ca ion concentration via dissolution of the filter materials the conductivity increases as well [28]. Because the increase of conductivity by Ca^{2+} is linked with the change in the concentration of HCO_3^-, the change in conductivity is also linked with the change in buffer capacity of the water. Instead of the Ca concentration and alkalinity, the conductivity is an easily measurable parameter and might be used for monitoring and control of the deacidification process.

3.3. Consumption of filter material

As intended, the limestone media were partly dissolved during deacidification filtration, so the filters were refilled every two weeks to maintain a consistent fill level over time. The target value for total alkalinity in the effluent was 2.0 mmol/L, which was exceeded in the pilot tests (Table 4), starting from 0.7 mmol/L in the mixed raw water. The effluent from the more reactive porous limestone exceeded the targeted value slightly more (2.6 mmol/L on average) than the dense limestone (average 2.4 mmol/L) resulting in greater consumption and the need for more frequent refilling of the porous limestone filter material.

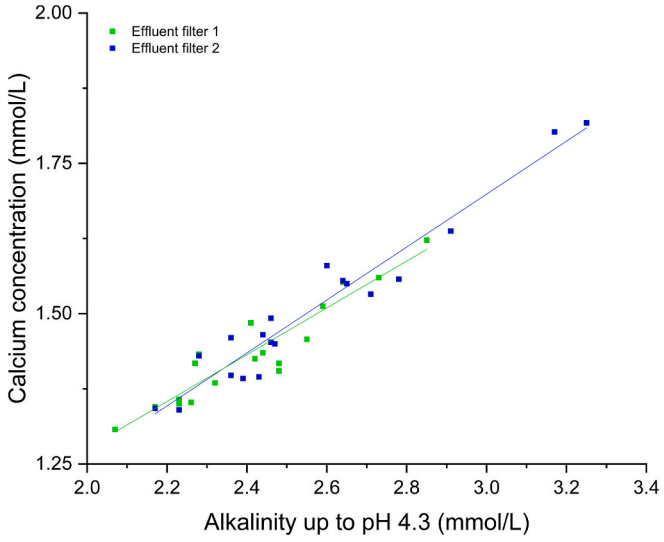

Fig. 7. Calcium concentration vs. alkalinity. Slopes of linear fits are 0.44 for Hydro-Calcit (blue line) and 0.39 for Jura Perle (green line).

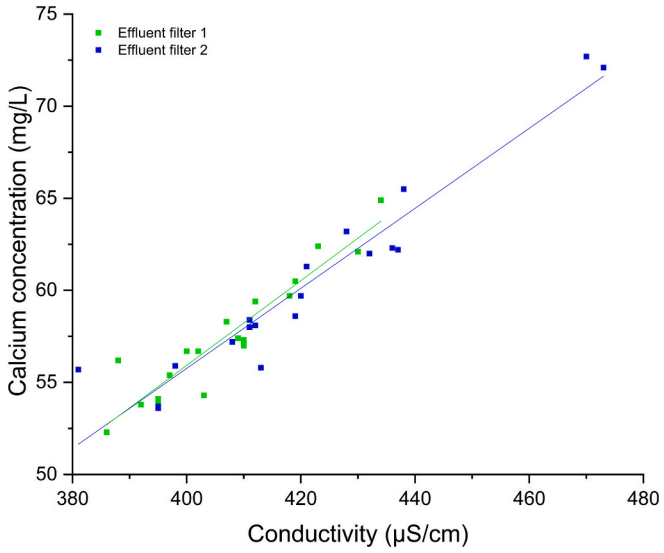

Fig. 8. Calcium concentration vs. conductivity.

3.4. Quality of spent backwash water

Spent backwash water was collected, allowed to settle, and the supernatant was sampled after 2 and 24 h. Sedimented sludge was dried, acid-neutralized, and subsequently analyzed for heavy metals. Despite the absence of flocculants or flocculation aids, the supernatant exhibited low turbidity, indicating that the sludge produced was readily settleable (Table 5). The concentrations of major cations in the supernatant (for example, magnesium) were similar to those in the raw water and are thus considered uncritical. In samples taken after Fe(II) dosing, the total chromium concentration in the supernatant was slightly elevated compared to samples without Fe(II)-dosage, but remained in the same range as raw water, making it irrelevant for direct or indirect discharge as wastewater. Because chromium concentrations were not elevated in the supernatant, the fate of chromium is expected to be in the sedimented sludge. Iron concentrations in the supernatant were unaffected by Fe(II) dosing. Recycling the supernatant upstream of the Fe(II) dosing

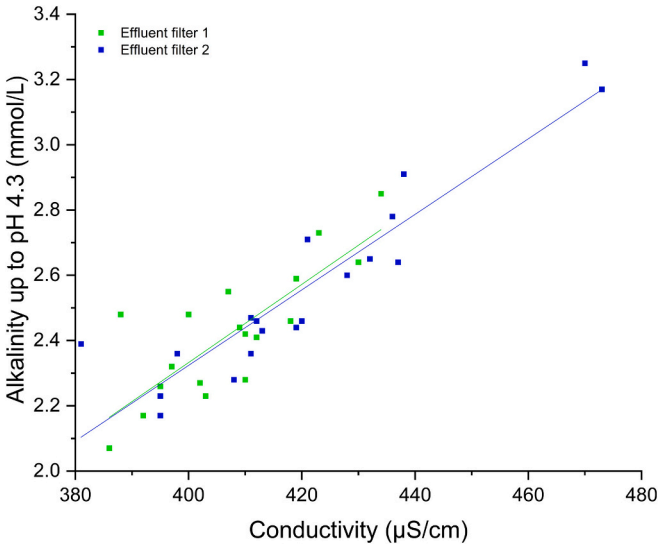

Fig. 9. Total alkalinity in filter effluents vs. conductivity.

Table 4
Filter material consumption and increase of total alkalinity.

	Unit	Filter one dense limestone Jura Perle	Filter two Porous limestone hydro-Calcit
Refill mass	kg	131	195
Treated water volume	m^3	1451	1473
Specific refill quantity	g/m^3	90	132
Mean total alkalinity after filtration	mmol/L	2.4	2.6

Table 5
Quality of supernatant from spent backwash water after sedimentation.

Parameter	Unit						
Filter		1	2	1	2	1	2
Phase		2	2	3	3	3	4
Fe(II)-dosage		No	No	Yes	Yes	Yes	Yes
pH	–	#NA	#NA	7.8	7.8	7.6	7.5
Conductivity	µS/cm	#NA	#NA	367	379	392	420
Turbidity	FNU	#NA	#NA	4.0	4.8	1.5	1.2
Chromium	mg/L	1	<0.5	2	2	4	3
Iron	mg/L	<0.01	0.08	0.10	<0.01	0.30	0.02
Calcium	mg/L	60	74	48	52	58	62
Magnesium	mg/L	5.8	6.0	6.2	5.7	6.6	5.9
Aluminum	mg/L	<0.01	0.05	<0.01	<0.01	0.12	0.11
Lead	mg/L	<2	<2	<2	<2	<2	<2
Cadmium	mg/L	<0.2	<0.2	<0.2	<0.2	<0.2	<0.2
Copper	mg/L	4	16	2	<0.2	60	10
Nickel	mg/L	<2	<2	<2	<2	<2	<2

is feasible without compromising filter effluent quality, especially no chromium concentration increase is expected if supernatant is recycled. Other heavy metal concentrations in the supernatant were low and deemed uncritical.

Analysis of the sedimented sludge (Table 6) showed that calcium was the dominant component, primarily resulting from abrasion of the filter material during backwashing. When Fe(II) was dosed, iron became the second most abundant constituent, due to precipitation during the process; otherwise, aluminum followed calcium in abundance. As expected, total chromium contents were highest with Fe(II) dosing, as chromium was precipitated after the reduction of Cr(VI) to Cr(III) during the RCF process [29]. If Cr(III) and Fe(III) occur alongside each other, Cr

Table 6
Quality of sedimented sludge from spent backwash water.

Filter		1	1	1	2	2
Phase		2	3	3	3	4
Fe(II)-dosage		No	Yes	Yes	Yes	Yes
Chromium	mg/kg	26	191	483	23	13
Iron	mg/kg	6500	6340	2020	8700	4600
Calcium	mg/kg	450,000	380,000	288,000	442,000	456,000
Magnesium	mg/kg	2700	2600	2900	4500	5800
Aluminum	mg/kg	11,300	10,600	14,100	600	900
Lead	mg/kg	27	23	46	9	9
Cadmium	mg/kg	0	2	4	0	0
Copper	mg/kg	98	460	1020	67	61
Nickel	mg/kg	17	16	26	<2.3	<2.8

(III) is co-precipitated within ferric hydroxide [23]. There was no evidence of chromium remobilization by dissolution or of reoxidation from Cr(III) to Cr(VI) after co-precipitation; chromium remained strongly bound in the co-precipitate with Fe(III) as described by Mahringer et al. [29]. In addition to chromium, copper was also co-precipitated with or adsorbed onto ferric hydroxide during the RCF process.

4. Conclusions

This study investigated the simultaneous removal of Cr(VI) and deacidification in a combined treatment process consisting of RCF with limestone filtration. The key findings are summarized as follows:

Cr(VI) removal via RCF

The RCF process achieved near-complete Cr(VI) removal (> 95%) when sufficient Fe(II) was dosed (e.g. 0.9 mg/L Fe(II)). Cr(VI) was rapidly reduced to Cr(III) and co-precipitated with Fe(III), with no observed breakthrough or reoxidation. Under optimal conditions (Fe(II) dosage: 0.9 mg/L, filtration velocities ≤13.3 m/h) effluent Cr(VI) concentrations remained below the detection limit (≤ 0.02 µg/L). In high-load scenarios with comparably low Fe(II) dosages and high filtration velocities (Cr(VI) > 5 µg/L in raw water, Fe(II) dosage ≤0.4 mg/L, filtration velocities ≥15.5 m/h) incomplete reduction led to residual Cr (VI) (1.0–1.5 µg/L) in the effluent, emphasizing the need for adequate Fe (II) dosing or extended contact time before filtration.

Effluent iron concentrations were consistently below 50 µg/L (German drinking water limit). Turbidity remained low (< 0.1 FNU), confirming effective biotic Fe(II) oxidation and filtration independent from filtration velocity.

Deacidification via limestone filtration

Both dense (Jura Perle) and porous (Hydro-Calcit) limestone filters significantly increased effluent pH (from ca. 6.0 to ca. 7.5), total alkalinity (from ca. 0.7 to more than 2.0 mmol/L), and calcium concentration (from ca. 22 to ca. 60 mg/L). Hydro-Calcit exhibited higher reactivity, yielding greater increases in alkalinity and calcium dissolution. CO_2 dosing prior to filtration enhanced limestone dissolution, further increasing buffer capacity.

Process monitoring and optimization

Conductivity correlated strongly with calcium concentration and total alkalinity, suggesting its suitability for real-time monitoring of deacidification and process control.

Limestone filtration (with short contact time) plus mechanical deacidification have proven to be a good combination to achieve a sufficiently high pH and a low calcite dissolution capacity in order to comply with the German drinking water regulations. Backwash water supernatant exhibited low turbidity (< 5 FNU) and chromium concentrations similar to raw water, enabling safe discharge or reuse. Sludge analysis confirmed Cr(III) immobilization in Fe(III)-rich precipitates, with no evidence of remobilization or reoxidation.

This study demonstrates the feasibility of integrating Cr(VI) removal and deacidification into a single treatment step, providing a cost-effective and scalable approach for regions facing co-occurring chromium contamination and acidic groundwater.

Declaration of generative AI and AI-assisted technologies in the manuscript preparation process

Statement: During the preparation of this work the authors used DeepSeek (2024)(DeepSeek Chat (Version 3) [Large language model]. https://www.deepseek.com) in order to improve the writing process and the readability of the manuscript. After using deepseek, the authors reviewed and edited the content as needed and take full responsibility for the content of the published article.

Funding sources

This pilot plant study was funded by a German water utility that wants to build a new waterworks including treatment processes for chromium removal and deacidification.

Declaration of competing interest

The authors declare that they have no known competing financial interests or personal relationships that could have appeared to influence the work reported in this paper.

Acknowledgements

For her great support with the figure editing we thank Nelly Delavernhe.

Appendix A. Supplementary data

Supplementary data to this article can be found online at https://doi.org/10.1016/j.seppur.2026.138507.

Data availability

Data will be made available on request.

References

[1] R.J. Bartlett, Chromium cycling in soils and water: links, gaps, and methods, Environ. Health Perspect. 92 (1991) 17–24, https://doi.org/10.1289/ehp.919217.
[2] J. Barnhart, Occurrences, uses, and properties of chromium, Regul. Toxicol. Pharmacol. 26 (1997) S3–S7, https://doi.org/10.1006/rtph.1997.1132.
[3] WHO, Chromium in drinking-water - Background document for development of WHO Guidelines for drinking-water quality, World Health Organization, Geneva, Switzerland, https://apps.who.int/iris/bitstream/handle/10665/338062/WHO-HEP-ECH-WSH-2020.3-eng.pdf, 2020.
[4] EU, Directive (EU) 2020/2184 of the european parliament and of the council of 16 December 2020 on the quality of water intended for human consumption, 2020.
[5] BMG, Ordinance on the Quality of Water intended for Human Consumption (Drinking Water Ordinance), 2023.
[6] California Water Boards, State Water Board Approves Removal of Drinking Water Standard for Hexavalent Chromium - Action Fulfills Court Order; Board to Create New Standard. https://www.waterboards.ca.gov/drinking_water/certlic/drinkingwater/Chromium6.shtml, 2024.
[7] C.M. Thompson, J.E. Rager, M. Suh, C.L. Ring, D.M. Proctor, L.C. Haws, R.C. Fry, M.A. Harris, Transcriptomic responses in the oral cavity of F344 rats and B6C3F1 mice following exposure to Cr(VI): Implications for risk assessment: Transcriptomic responses in the oral cavity, Environ. Mol. Mutagen. 57 (2016) 706–716, https://doi.org/10.1002/em.22064.
[8] I. Moffat, N. Martinova, C. Seidel, C.M. Thompson, Hexavalent chromium in drinking water, J. Am. Water Works Assoc. 110 (2018) E22–E35, https://doi.org/10.1002/awwa.1044.
[9] N.N. Ramli, S.B. Kurniawan, J.O. Ighalo, N.S. Mohd Said, N. Marsidi, J. Buhari, R. A. Ramli Shah, M. Zulkifli, J. Alias, N.M. Daud, J. Ahmad, A.R. Othman, S. R. Sheikh Abdullah, H. Abu Hasan, A review of the treatment technologies for hexavalent chromium contaminated water, BioMetals 36 (2023) 1189–1219, https://doi.org/10.1007/s10534-023-00512-x.
[10] N. Blute, X. Wu, C. Cron, R. Abueg, D. Froelich, L. Fong, Hexavalent chromium treatment implementation in Glendale, Calif. J. - Am. Water Works Assoc. 106 (2014) E160–E175, https://doi.org/10.5942/jawwa.2014.106.0022.
[11] N. Konradt, S. Dillmann, J. Becker, D. Schroden, H.-P. Rohns, C. Wagner, U. Müller, D. Konradt, P. Janknecht, R. Hobby, I.M.A. ElSherbiny, S. Panglisch, Removal of chromium species from low-contaminated raw water by different drinking water treatment processes, Water 15 (2023) 516, https://doi.org/10.3390/w15030516.
[12] A.R. Asgari, F. Vaezi, S. Nasseri, O. Dördelmann, A.H. Mahvi, E. Dehghani Fard, Removal of hexavalent chromium from drinking water by granular ferric hydroxide, J. Environ. Health Sci. Eng. 5 (2008) 277–282.
[13] K. Johannsen, Kapitel 7, Stabilisierung, in: S. Panglisch, R. Winzenbacher (Eds.), Wasseraufbereit. – Grundlagen Verfahr. Water Treat. – Fundam. Process, 3rd ed., Springer Vieweg, Wiesbaden, 2025.
[14] DVGW, pH-Adjustment in Drinking Water Treatment; Part 1: Principles and Methods, 2016 doi:ISSN:%200176–3504.
[15] DVGW, pH-Adjustment in Drinking Water Treatment; Part 5: Pretreatment of very soft and very acidic Waters, 2017 doi:ISSN:%200176–3504.
[16] I.J. Buerge, S.J. Hug, Kinetics and pH dependence of chromium (VI) reduction by iron (II), Environ. Sci. Technol. 31 (1997) 1426–1432, https://doi.org/10.1021/es960672i.
[17] D.L. Sedlak, P.G. Chan, Reduction of hexavalent chromium by ferrous iron, Geochim. Cosmochim. Acta 61 (1997) 2185–2192, https://doi.org/10.1016/S0016-7037(97)00077-X.
[18] D. Mahringer, C. Polenz, F. El-Athman, Stabilization of chromium (VI) in the presence of iron (II): method development and validation, Water 12 (2020) 924, https://doi.org/10.3390/w12040924.
[19] S.E. Fendorf, G. Li, Kinetics of chromate reduction by ferrous iron, Environ. Sci. Technol. 30 (1996) 1614–1617, https://doi.org/10.1021/es950618m.
[20] M. Pettine, L. D'Ottone, L. Campanella, F.J. Millero, R. Passino, The reduction of chromium (VI) by iron (II) in aqueous solutions, Geochim. Cosmochim. Acta 62 (1998) 1509–1519, https://doi.org/10.1016/S0016-7037(98)00086-6.
[21] Z. Zhu, H. Yang, J. Liu, Y. Zhu, S. Tang, L. Zhang, X. Wang, Dissolution, solubility, and stability of the basic ferric sulfate-arsenates [Fe(SO4)x(AsO4)y(*OH*)z·nH2O] at 25–45 °C and pH 2–10, J. Chemother. 2021 (2021) 1–14, https://doi.org/10.1155/2021/5556295.
[22] R. Gimbel, M. Jekel (Eds.), Wasseraufbereitung - Grundlagen und Verfahren, Oldenbourg Industrieverl, München, 2004.
[23] B.M. Sass, D. Rai, Solubility of amorphous chromium(III)-iron(III) hydroxide solid solutions, Inorg. Chem. 26 (1987) 2228–2232, https://doi.org/10.1021/ic00261a013.
[24] BMG, German Drinking Water Ordinance, 2023.
[25] B. Morgan, O. Lahav, The effect of pH on the kinetics of spontaneous Fe(II) oxidation by O2 in aqueous solution – basic principles and a simple heuristic description, Chemosphere 68 (2007) 2080–2084, https://doi.org/10.1016/j.chemosphere.2007.02.015.
[26] P. Grothe, C. Czekalla, Enteisenung und Entmanganung, in: R. Gimbel, M. Jekel, Deutsche Vereinigung des Gas- und Wasserfaches (Eds.), Wasseraufbereit. - Grundlagen Verfahr., Oldenbourg Industrieverl, München, 2004.
[27] D. Mahringer, M. Lutz, M. Klumbies, S. Pabst, A.S. Ruhl, Reduction, coagulation and biotic filtration (RCbF) for Cr(VI) groundwater remediation – A case study, J. Water Process Eng. 65 (2024) 105867, https://doi.org/10.1016/j.jwpe.2024.105867.
[28] Y.P. Ingin, D. Mahringer, F. El-Athman, Hardness properties of calcium and magnesium ions in drinking water, Appl. Food Res. 4 (2024) 100600, https://doi.org/10.1016/j.afres.2024.100600.
[29] D. Mahringer, S.S. Zerelli, U. Dippon, A.S. Ruhl, Pilot scale hexavalent chromium removal with reduction, coagulation, filtration and biological iron oxidation, Sep. Purif. Technol. 253 (2020) 117478, https://doi.org/10.1016/j.seppur.2020.117478.